

## Supplemental material

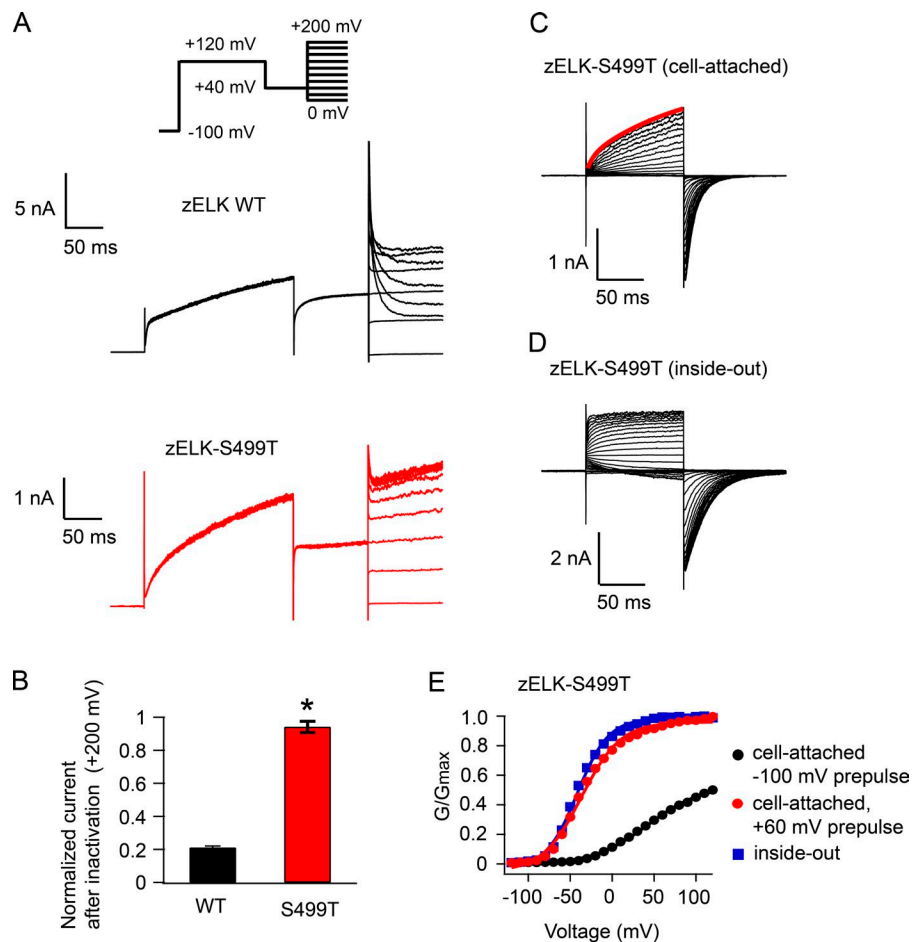
Dai et al., <https://doi.org/10.1085/jgp.201711989>

Figure S1. **S499T mutation abolished the inactivation of zELK channels.** (A) Representative current traces elicited by a three-component voltage protocol, consisting of a +120-mV depolarizing pulse from the resting -100 mV, a +40-mV pulse for the recovery of the inactivation, and a family of depolarizing voltage steps from 0 to +200 mV to visualize the inactivation, which is unmasked by the recovery pulse. S499T removed the inactivation almost completely. (B) Summary of the current amplitude at the end of the +200-mV pulse in the family of voltage steps in A, normalized to the peak of the current amplitude in the beginning of the +200-mV voltage pulse, for zELK wild-type and zELK-S499T channels ( $n = 4$ ).  $^*$ ,  $P < 0.01$ . (C) Representative I-V traces for the activation of zELK-S499T channels in the cell-attached configuration using the voltage protocol in Fig. 1 B. The red curve is the fit of the current activation at +120 mV by a double-exponential function with  $\tau_1 = 6.4$  ms and  $\tau_2 = 103$  ms. (D) Representative I-V traces for the activation of zELK-S499T channels after run-up in the inside-out configuration using the same voltage protocol in C. (E) G-V curve of the zELK-S499T channel activation in the control cell-attached configuration ( $V_{1/2} = 38$  mV), after a +60-mV prepulse ( $V_{1/2} = -37$  mV), and after run-up ( $V_{1/2} = -41$  mV).

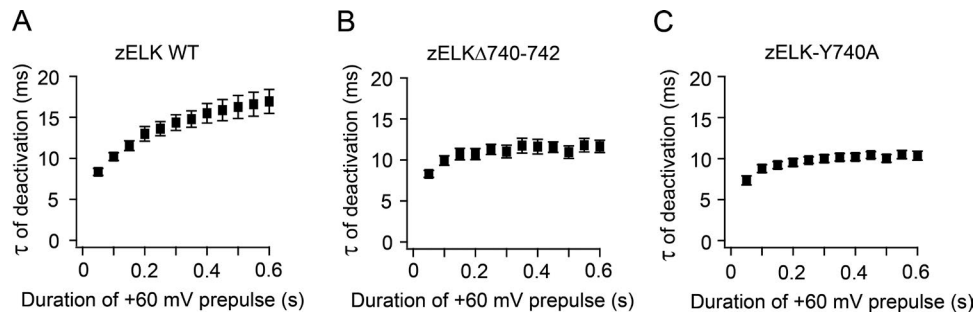


Figure S2. **Summary of the time constants of the tail currents.** Summary of the time constants of the tail current using the protocol in Fig. 2 C for zELK wild-type ( $n = 12$ ; A), zELK $\Delta$ 740–742 ( $n = 5$ ; B), and zELK-Y740A channels ( $n = 5$ ; C). Data are shown as mean  $\pm$  SEM.

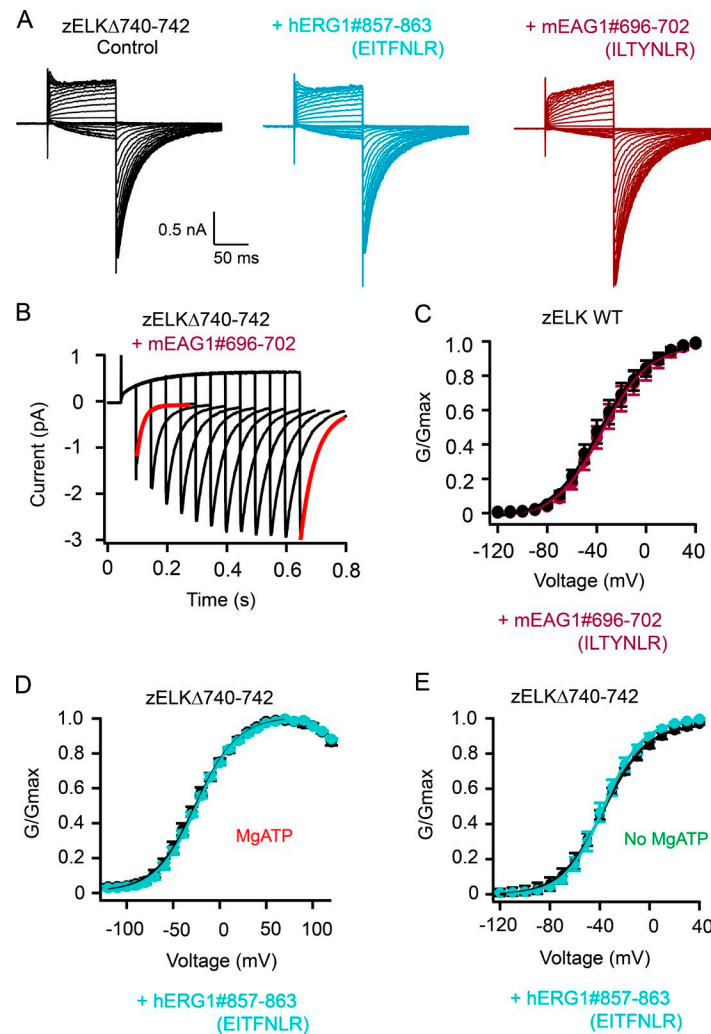


Figure S3. **Effects of the intrinsic-ligand peptide.** (A) Representative I-V traces for the activation of zELK $\Delta$ 740–742 channels before and after adding hERG1 and mEAG1 peptides, all in the presence of MgATP. (B) Current traces of zELK $\Delta$ 740–742 channels after applying the mEAG1 peptide, elicited by a voltage protocol with increasing durations of +60-mV pulse in the presence of MgATP. (C) The intrinsic-ligand peptide from hEAG1 did not significantly affect the voltage-dependent gating of zELK wild-type channels in the absence of MgATP. (D) The intrinsic-ligand peptide from hERG1 did not significantly affect the voltage-dependent gating of zELK $\Delta$ 740–742 channels in the presence of MgATP. (E) The intrinsic-ligand peptide from hERG1 did not significantly affect the voltage-dependent gating of zELK $\Delta$ 740–742 channels in the absence of MgATP. Data are shown as mean  $\pm$  SEM,  $n = 3$ –5.

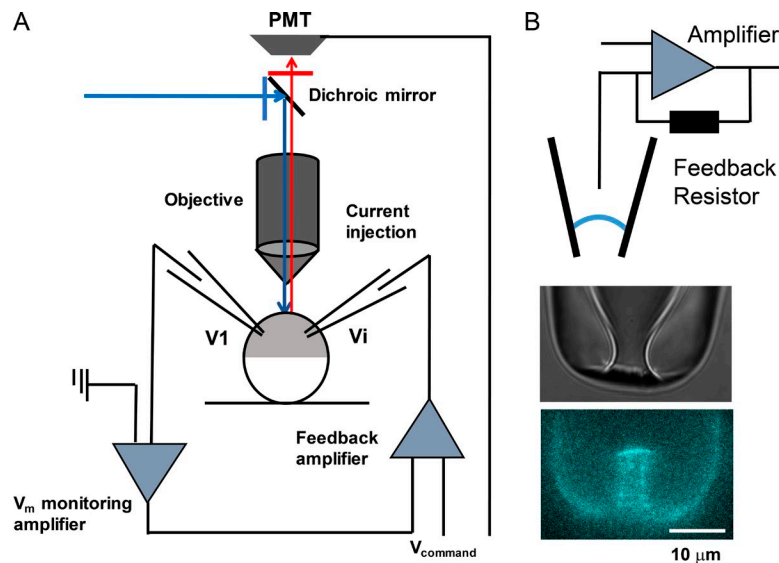


Figure S4. **Comparison of PCF and VCF.** (A) Diagram showing the design of VCF. The oocyte is voltage clamped with a two-electrode voltage-clamp amplifier.  $V_i$  is the microelectrode for current injection, and  $V_1$  is the microelectrode for monitoring membrane voltages. PMT, photomultiplier tube. (B) Diagram illustrating PCF. The upper image is a giant patch electrode in brightfield, whereas the lower image shows the L-Anap fluorescence from the same patch.

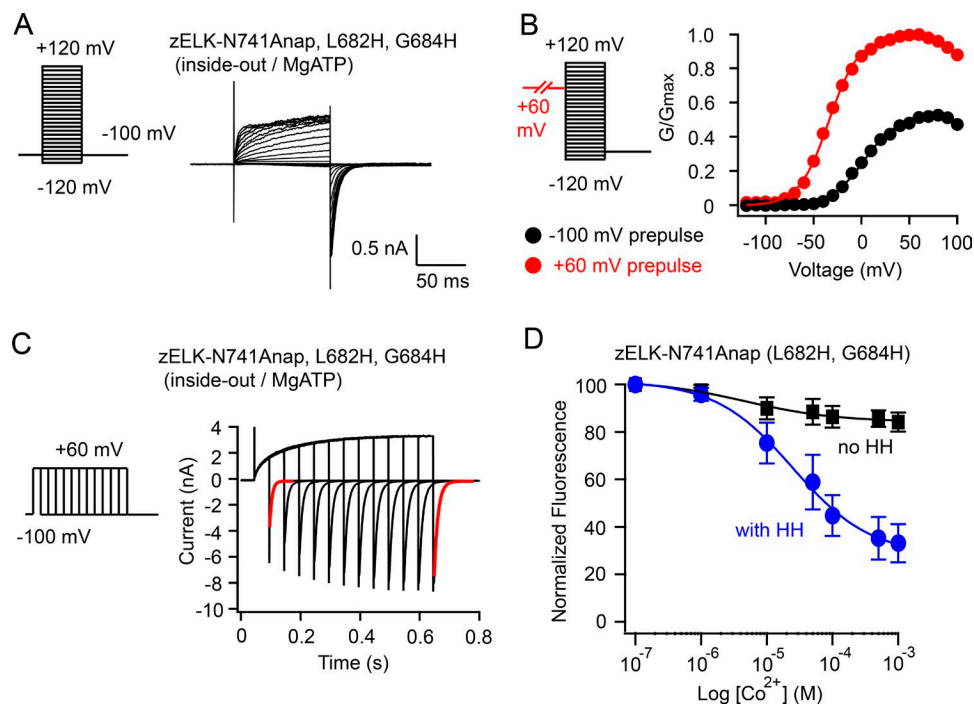


Figure S5. **Properties of zELK-N741Anap channels.** (A) Representative I-V recordings for zELK-N741Anap, L682H, G684H channel activation in the inside-out configuration using the voltage protocol with steps of depolarizing voltages. MgATP is present in the bath solution. (B) G-V curve of zELK-N741Anap, L682H, G684H activation with ( $V_{1/2} = -34$  mV) and without ( $V_{1/2} = 2$  mV) the 500-ms, +60-mV prepulse. (C) Currents of zELK-N741Anap, L682H, G684H channels elicited by a voltage protocol with increasing durations of a +60-mV pulse.  $\tau$  of the tail current recovery (red traces) increased from 7 to 13 ms. (D) Quenching of Anap fluorescence measured using PCF by different concentrations of  $Co^{2+}$  with or without dihistidines and in the presence of 2 mM MgATP at the resting holding voltage of -100 mV. Data are shown as mean  $\pm$  SEM,  $n = 4$ .

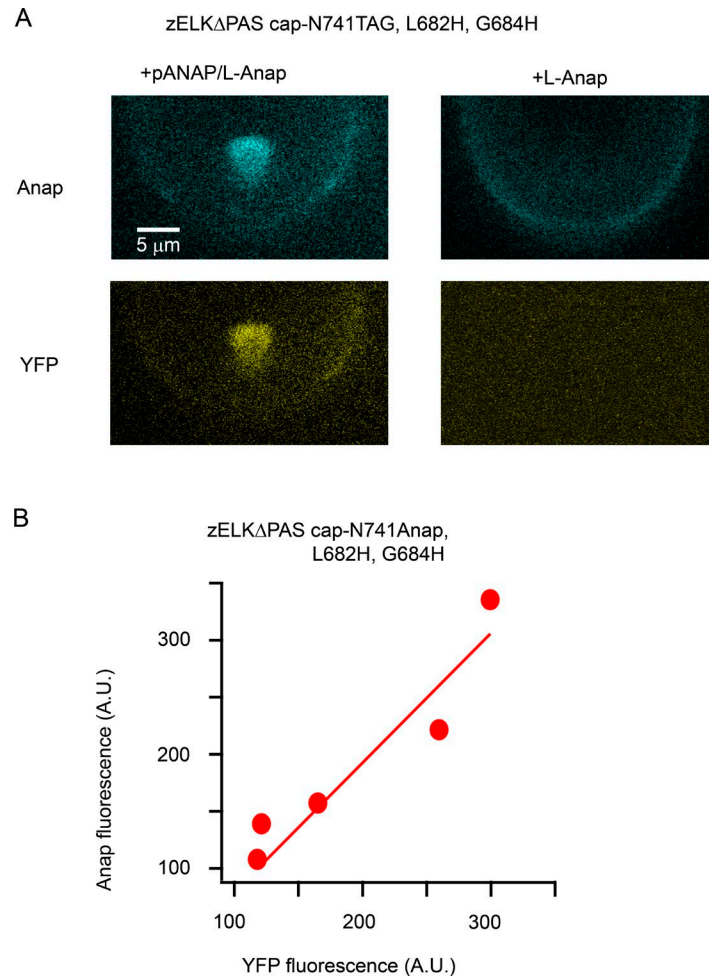


Figure S6. **Successful incorporation of Anap for zELKΔPAS cap-N741TAG,L682H,G684H channels.** **(A)** Representative PCF images with oocytes injected with mRNA of zELKΔPAS cap-N741TAG,L682H,G684H, L-Anap, and with (left) or without (right) pANAP vector. **(B)** Relationship of Anap fluorescence versus YFP fluorescence measured by PCF for zELKΔPAS cap-N741Anap,L682H,G684H channels. A.U., arbitrary units.